Wood Terpenes as Bio-based Monomers in Latex for Sustainable Coatings

Maylis Carrère,[a] Stéphane Beaupré,[b] Yvan Ecochard,[b] and Véronic Landry [a,c,*]

Recent global market disruptions, including the COVID-19 crisis, inflation, and oil crises, have highlighted the need for industries to reduce dependence on petrochemicals. However, the coating industry remains reliant on petrochemicals due to a lack of knowledge about local and sustainable alternatives. This study explored the potential of wood extractives as precursors for producing high-quality wood coatings. Terpenes were modified through acrylation, and bio-based latexes were synthesized from these modified terpenes. Analysis showed that all tested latexes had conversion levels above 88.5%. The bio-based films were characterized, and their transparency, measured by ultraviolet-visible spectroscopy, exceeded 80%. The good incorporation of bio-based monomers in the latex films was confirmed by thermogravimetric analysis and pyrolysis-gas chromatography-mass spectrometry. Comparative analysis between bio-based and conventional latexes showed equivalent results in particle size, molecular weight, glass transition temperature, and minimum film formation temperature. However, bio-based films exhibited lower hardness. The study suggests that using monomers derived from wood extractives offers a viable alternative to petrochemicals, utilizing abundant forest residues. This approach could address raw material shortages and help make the coatings industry more sustainable by reducing its reliance on petrochemicals.

DOI: 10.15376/biores.19.3.6510-6529

Keywords: Terpene; Waterborne coating; Acrylic monomers; Latex; Miniemulsion

*Contact information: a: Department of Wood and Forest Sciences, NSERC Industrial Research Chair on Eco-Responsible Wood Construction (CIRCERB), Université Laval, Québec, QC G1V 0A6, Canada; b: MAPEI INC., Laval, Québec, H7L 3J5, Canada; c: Department of Wood and Forest Sciences, NSERC Canlak Industrial Research Chair in interior Wood-Products Finishes, Université Laval, Québec, QC G1V 0A6, Canada; *Corresponding author: veronic.landry@sbf.ulaval.ca*

INTRODUCTION

Building with wood offers numerous advantages. These include a favorable strength-to-weight ratio, the ability to create lighter structures, improved mental health and well-being for occupants (Ulrich 1983), and the potential to reduce greenhouse gas emissions when forests are managed sustainably (Lippke *et al.* 2011). Nevertheless, the wood must be preserved from deterioration, especially when exposed to exterior conditions. One of the preferred means to protect wood is the application of coatings. In the coating and chemical industry, one of the greatest challenges is reducing the use of petrochemicals (Sainz *et al.* 2016). The use of petrochemicals in the coatings industry is linked to the extensive use of petroleum-derived raw materials, particularly as solvents. This leads to significant volatile organic compounds (VOCs) emissions, contributing to greenhouse gas (GHG) emissions.

The paint industry has started to adopt new technologies because of environmental pressures. For example, in Canada, over the last 30 years, there has been a shift from solvent-based to water-based paints due to rising concerns over VOCs emissions. Advances in acrylic binders, waterborne resins, and thickening technologies have facilitated this transition (González-Laredo *et al.* 2015). Petroleum-based (meth)acrylic polymers are widely used in the development of water-based wood coatings due to their favorable properties (Jiao *et al.* 2021), in particular, their resistance to photodegradation (Jones *et al.* 2017). In addition, acrylic latex films are more permeable to water than oil or alkyd paints, which is an advantage for wood applications as it reduces blistering, cracking, chalking, and erosion (Jones *et al.* 2017). Latexes are produced using hard monomers, such as methyl methacrylate (MMA), whose homopolymers have a high glass transition temperature (T_g(Poly(MMA)) = 105 °C) (Jones *et al.* 2017) and soft monomers, such as butyl acrylate (T_g(Poly(BuA)) = -54 °C) (Jones *et al.* 2017), whose homopolymers have a low T_g, and stabilizing monomers such as acrylic acid (T_g(Poly(AA)) = 101 °C) (Désor *et al.* 1999; Jones *et al.* 2017). The glass transition temperature (T_g) of the final film and the minimum film forming temperature (MFFT) must be controlled to ensure good performance in service. In the case of exterior coatings, the expected T_g should be between 3 and 10 °C (Jones *et al.* 2017). Coatings must be able to be applied even when the outside temperature is low, *i.e.*, below 10 °C.

To further advance the environmental approach aligned with the sought performance, bio-based polymers can be used to prepare coatings. These bio-based solutions must be environmentally friendly and excel in performance and cost-effectiveness, while meeting performance standards similar to those of petroleum-based polymers. However, developing bio-based polymers that meet these criteria remains a major challenge. Moreover, it is important to explore using locally available bio-based materials to adhere to green chemistry principles (Anastas and Eghbali 2010) and mitigate concerns regarding raw material scarcity.

Terpenes stand out among the various sources of bio-based molecules available for protecting exterior wood products. In addition to their polymerization potential, terpenes and terpenoids possess antifungal and antibacterial properties (Demurtas *et al.* 2023), which make them particularly interesting for use as components of exterior wood finishes. They are abundant in softwood and can be extracted from wood waste as turpentine. Turpentine can also be obtained as a byproduct of the paper industry during the kraft softwood pulping (Donoso *et al.* 2021). The North American region dominates the global crude sulfate turpentine (CST) market, commanding a substantial 60.64% share in CST production. Turpentine mainly consists of monoterpenes, primarily α-pinene, and β-pinene, with smaller amounts of D-limonene, camphene, and myrcene (Izmest'ev *et al.* 2019). Due to their isoprenic chemical structure, terpenes can participate in various types of polymerization reactions, including radical polymerization, and polymerization processes such as emulsion polymerization (Belgacem and Gandini 2011). Furthermore, their chemical structures allow them to be functionalized into (meth)acrylates.

Myrcene-derived terpenoids such as tetrahydrogeraniol (THG) and citronellol have promising chemical structures with an 8-carbon chain terpenoid with a hydroxyl group. TH is well known for its acrylation in scientific literature. Noppalit *et al.* (2019) conducted research on THG, a byproduct from the paper industry, to investigate its potential as a bio-based acrylate precursor for producing triblock copolymers. They utilized the low T_g of poly(tetrahydrogeraniol acrylate) (poly-THGA; -46 °C) to create the soft segments of their elastomers; styrene was selected as the monomer for the hard segment. Castagnet *et al.*

(2020) worked on an environmentally friendly method based on bioinspired enzymatic catalysis to synthesize a new set of (meth)acrylic monomers from terpenoids extracted from wood biomass. In addition, several studies had already polymerized THGA in emulsion. Droesbeke *et al.* (2018) recently produced bio-based pressure-sensitive adhesives (PSA) using terpenoids, specifically THGA and citronellyl (meth)acrylate. As a result of the high THGA content, most of the materials synthesized *via* emulsion polymerization display low T_g values.

Isobornyl methacrylate (IBOMA) is a monomer synthesized from the terpenoid borneol, a derivative of camphene. Sun *et al.* (2016) already used borneol acrylate to develop a new copolymer composed of methyl methacrylate and borneol acrylate that can effectively prevent bacterial adhesion. Poly(IBOMA) is a high T_g homopolymer (with literature values ranging from 140 to 195 °C) (Hadjichristidis *et al.* 1984; Zhang *et al.* 2013) that can potentially replace methyl methacrylate in waterborne formulations. Indeed, the T_g of the homopolymer being high, IBOMA can be the so-called hard monomer.

A few papers have reported the possibility of synthesizing bio-based latexes from bio-based monomers. The raw material has acrylate or methacrylate functions for the monomers to participate in the emulsion polymerization. The targeted applications highlighted in the literature are pressure-sensitive adhesives and coatings. For example, Fang *et al.* (2020) evaluated IBOMA as an alternative to traditional petroleum-based MMA as a hard monomer for acrylic latex PSA. Baek *et al.* (2017) used THGA to make transparent, UV-cured acrylic PSAs composed of semi-interpenetrating networks. Badia *et al.* (2018) used two partially bio-based commercial monomers of 2-octyl acrylate (derived from castor oil) and IBOMA copolymerized by emulsion polymerization. These latexes showed promising adhesive properties.

Gonzalez *et al.* (2021) polymerized IBOMA and 2-octyl acrylate by mini-emulsion polymerization for bio-based latexes intended for coating applications and obtained excellent anticorrosive properties. Allasia *et al.* (2022) synthesized bio-based aqueous latexes by emulsion polymerization incorporating IBOMA and 2-octyl acrylate in the presence of methacrylated casein (bovine milk protein). The resulting films showed promising mechanical properties, solvent resistance, and biodegradability in organic compost, which could pave the way for synthesizing binders with a high biological raw material content for waterborne coatings. Llorente *et al.* (2022) incorporated large amounts of the bio-based IBOMA monomer into an emulsion copolymerization reaction with the bio-based 2-octyl acrylate to produce high solids bio-based copolymer latexes.

This study focused on preparing latexes from terpene-derived monomers for outdoor wood coatings, considering the requirements for water-based latex exterior finishes. Copolymers were prepared following the guidelines of the Fox-Flory equation (Fox 1956), with a chosen T_g of 4 °C to ensure flexibility, crucial for adapting to outdoor variations. The selected terpenes were chosen based on their acrylation potential and the T_g of homopolymers of acrylated terpenes. THGA was synthesized from THG, and the commercial version of IBOMA was utilized. The primary objective was to generate different types of latex preparations: conventional, semi-bio-based, and bio-based. Mini-emulsion polymerization, selected due to IBOMA's highly hydrophobic nature, aimed for maximal incorporation of bio-based monomers, a goal facilitated by this process's effectiveness. Furthermore, mini-emulsion polymerization had been previously utilized with IBOMA. Subsequently, a comparison was drawn regarding their performance as coatings, highlighting the potential of terpene-derived monomers to replace traditional ones. The study encompassed latex production and characterization based on conventional

and bio-based monomers. Finally, films were prepared from these latexes, and their performance was evaluated.

EXPERIMENTAL

Latex Synthesis

Latexes were prepared from both petroleum-based and bio-based monomers. Conventional monomers used were methyl methacrylate (MMA, 99%, containing less than 30 ppm MEHQ as inhibitor), butyl acrylate (BuA, 99%, containing 10 to 60 ppm MEHQ as inhibitor), and acrylic acid (AA, anhydrous containing 200 ppm MEHQ as inhibitor) from Sigma Aldrich, Canada. Bio-based monomers used were isobornyl methacrylate (IBOMA, Visiomer® Terra IBOMA, 150 ppm MEHQ, Evonik, Canada) and tetrahydrogeraniol acrylate (THGA) synthesized from tetrahydrogeraniol (THG, 3,7-dimethyl-1-ol, > 98.0% Sigma Aldrich, Canada). Details of the synthesis and characterization of THGA are given in the supplementary information (see Appendix). The surfactant used was sodium dodecyl sulphate (SDS, BioReagent, > 98.5%). The co-stabilizer was made with hexadecane (ReagentPlus®, 99%, Sigma Aldrich, Canada). The initiator used was potassium persulphate (KPS, 99.99% trace metal base, Sigma Aldrich, St. Louis, MO, USA). The quantities of these compounds used for the synthesis are listed in Table 1, and chemical structures are shown in Figure 1.

Table 1. Compounds and Amounts Employed in the Synthesis of Acrylic Latexes

Part	Compounds	Amount (g)
Soft monomer	BuA and/or THGA	7 to 8
Hard monomer	IBOMA and/or MMA	4 to 6
Functional monomer	AA	1
Co-stabilizer	Hexadecane	0.14
Emulsifier	SDS	0.8
Initiator	KPS	0.03 to 0.04
Continuous phase	Deionized water	40

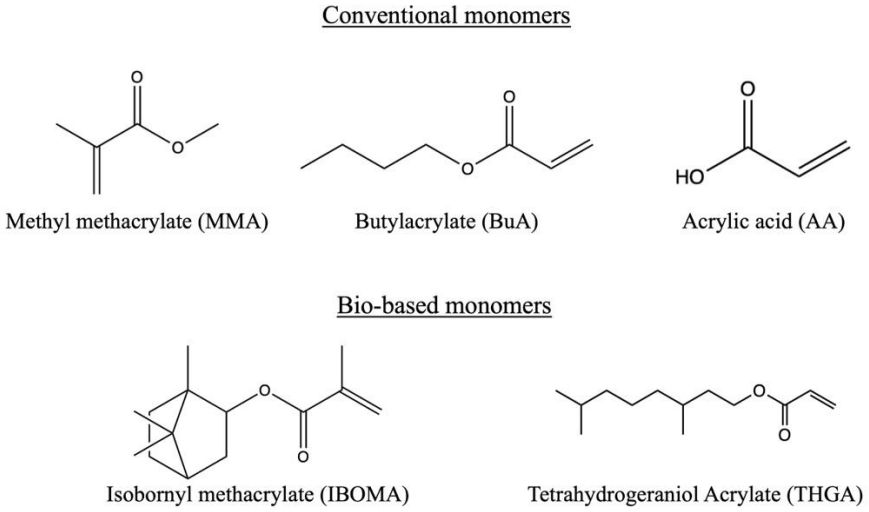

Fig. 1. Chemical structures of the monomers used in this study

Miniemulsion Polymerization

One of the most important parameters of latex films is their T_g. As the T_g is related to the percentage of each monomer used in the polymerization, the theoretical T_g of the final copolymer can be determined with the Flory-Fox equation (Fox 1956), given as Eq. 1,

$$\frac{1}{T_g} = \frac{w_1}{T_{g_1}} + \frac{w_2}{T_{g_2}} + \frac{w_3}{T_{g_3}} + \cdots \quad (1)$$

where w is the weight fraction of the monomers, and T_g is expressed in Kelvin.
The targeted theoretical T_g of the latexes was set to 4 °C. The T_g of 4 °C broadly keeps the proportions of rigid and soft monomers equivalent. The quantities of monomers used to construct the copolymer are listed in Table 1. Between the different latexes, the ratio of each monomer is adjusted using the T_g values found in the literature listed in Table 2.

Table 2. Glass Transition Temperatures (T_g) of Homopolymers

Homopolymers	T_g (°C)
Poly(MMA)	105 (Jones *et al.* 2017)
Poly(IBOMA)	140 to 195 (Llorente *et al.* 2022)
Poly(BuA)	-54 (Jones *et al.* 2017)
Poly(THGA)	-46 (Noppalit *et al.* 2019)
Poly(AA)	101 (Jones *et al.* 2017)

The corresponding monomer composition for each latex is given in Table 3 and was determined based on the homopolymers' T_g value. The value used for homopoly (IBOMA) was 173 °C. It was determined following the homopolymerisation of IBOMA and a DSC analysis presented in the supplementary information.

Table 3. Monomer Mass Percentage and Theoretical T_g for the Synthesized Latexes

Latex ID	Monomers	T_g theo (°C)	MMA (%)	BuA (%)	AA (%)	IBOMA (%)	THGA (%)
M1 Petrochemical	MMA:BuA:AA	4.2	42.8	50.0	7.1	-	-
SB2 Partially-bio-based	MMA:BuA:AA: IBOMA	4.6	7.4	55.9	7.4	29.4	-
SB3 Partially-Bio-based	MMA:BuA:AA THGA	4.3	39.8	21.8	7.5	-	30.8
B1 Highly Bio-based	MMA:AA:IBOMA: THGA	4.2	8	-	8	24.0	60

The protocol is illustrated in Fig 2. The monomers were mixed with hexadecane in a first beaker (b_1). The amount of hexadecane used corresponded to 1% of the total monomer mass. In another beaker (b_2), water and SDS were mixed. The amount of SDS corresponds to 2% of the amount of water. Then, b_2 was poured into b_1, stirring the mixture

for 20 min (Fig. 1-A). In parallel, a KPS solution in water was prepared. The amount of KPS was set to 0.25% of the monomer mass.

The obtained emulsion (b_2 + b_1) was placed under an ultrasound probe (CPX 750, 750 W, 20 kHz) set at 80% of its power during 3 min with alternating pulses of 1 s action and 1 s rest. The emulsion was then placed in a three-neck round bottom flask sealed with rubber seals, and the mixture was purged under nitrogen for 20 min, still under magnetic stirring (Fig. 2-B). The KPS solution was also bubbled under nitrogen.

The three-neck round bottom flask was then placed in an oil bath at 80 °C under stirring, and the mixture was kept under nitrogen. The reaction was then initiated by adding the KPS solution to the flask using a syringe. The reaction mixture was left in the bath to polymerize while stirring under nitrogen for 4 h (Fig. 2-C).

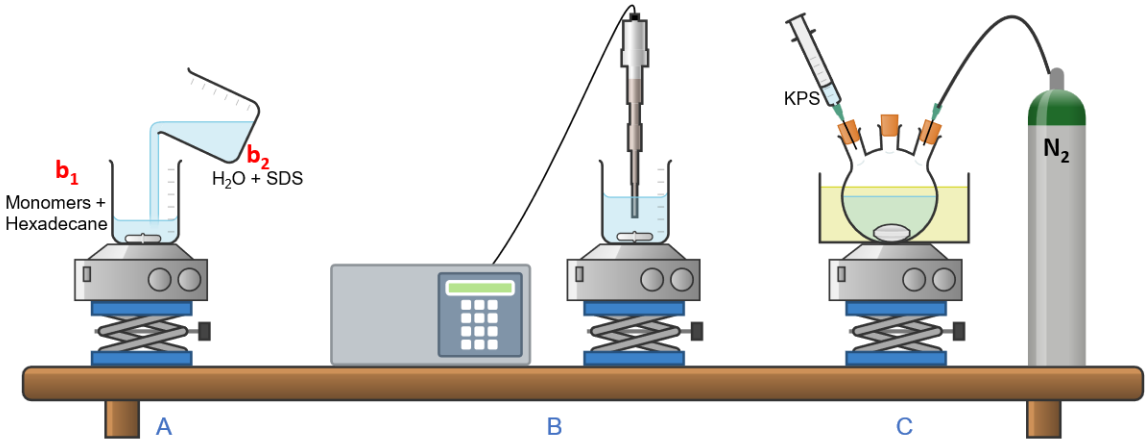

Fig. 2. Experimental protocol for miniemulsion polymerization, A – Stirring the pre-emulsion, B – Ultrasonication, C – Miniemulsion polymerization

Latex Characterization

Particle size

Latex particle size was determined using dynamic light scattering (DLS) (NanoBrook, Brookhaven Instruments Corporation). Analyses were carried out at 25 °C; each result averages ten successive measurements. To avoid clusters of particles during measurement, the latex was first diluted by a factor of 100 with nanopure water.

Solids content and conversion

The conversion percent was measured by gravimetric analysis. A total of 2 g of latex were weighed into an aluminum pan and dried in an HB43-S halogen oven (Mettler Toledo, Mississauga, Canada) to a constant weight. Solids content and the final conversion were calculated using Eq. 2,

$$\text{Conversion percent} = \frac{\%_{\text{solids content}} - \%_{\text{non volatiles compound}}}{\%_{\text{monomers at the beginning}}} \times 100 \quad (2)$$

where $\%_{\text{solids content}}$ corresponds to the mass percentage of solids obtained by gravimetry, $\%_{\text{non-volatiles compound}}$ is the mass percentage of SDS plus KPS, and $\%_{\text{monomers at the beginning}}$ is the percentage by weight of the total monomers used initially.

Gel permeation chromatography (GPC)

The weight average molecular weight (M_w) of the soluble fraction of polymer was determined using Gel Permeation Chromatography (GPC). The equipment included an Agilent 1200 (Agilent Technologies, Inc., Santa Clara, CA, USA), isocratic pump, detector: refractive index, column: PL Gel 5 µm, 300 x 7.5 mm^2, Guard column: PL Gel 5 µm, 50 x 7.5 mm^2. The method used involved injecting a volume of 50 µL with a column flow rate set at 0.5 mL/min. The chromatographic run lasted for 30 min, with an additional 5 min of post-injection time. The solvent used was 100% stabilized tetrahydrofuran (THF). Furthermore, the column temperature during the analysis was maintained at 40 °C. The results were interpreted using a calibration curve prepared from 12 polystyrene standards with molecular weights between 162 and 6,570,000 g/mol.

Film Characterization

Differential scanning calorimetry analysis (DSC)

The T_g of the latex films was determined using a differential scanning calorimeter (DSC 823, Mettler Toledo, Mississauga, Canada). The dry film was weighted (5 to 15 mg) into a standard DSC non-hermetic alumina crucible. To eliminate thermal history, two scanning cycles of heating-cooling were performed for each sample at a heating rate of 10 °C/min in the -50 to 80 °C range under a nitrogen atmosphere. The second heating run was used to determine the T_g.

Minimum film forming temperature analysis (MFFT)

The Rhopoint instrument model MFFT 60 (Rhopoint Americas Inc, Troy, MI, USA) was used to carry out measurements of MFFT. The MFFT was determined by averaging three temperatures across three runs, ranging from 0 to 18 °C.

Optical transparency

Latex films were prepared by pouring 5 g of latex into silicone moulds (5.5 cm x 8 cm). They were then placed in a ventilated oven at 50 °C for 12 h. The resulting films have a thickness of 300 µm. A ultraviolet-visible (UV-vis) spectrometer (Cary 60, Agilent Technologies, Inc., Santa Clara, USA) was used to study the optical transparency of the films obtained. The instrument was set to scan at wavelengths between 400 and 800 nm in transmittance mode.

Evaluation of water whitening of latex coatings

The water whitening protocol was inspired by the article from Machotová *et al.* (2018). Water whitening of the films was assessed by measuring the change in transmittance at a fixed wavelength (500 nm, close to the green light wavelength to which the human eye is most sensitive) using a UV-vis spectrometer (Cary 60, Agilent Technologies, Inc., Santa Clara, CA, USA). Before measurement, latexes were applied on microscope lamella at 20 mils wet. The films were left to dry overnight in a ventilated oven at 50 °C. An initial measurement was taken. Then, lamellas were immersed in distilled water at room temperature for 1 and 24 h, respectively, and the transmittance of the exposed area of the coating film was immediately measured. The degree of water bleaching *W* was given by Eq. 3,

$$W = \frac{100(T_0 - T_t)}{T_0} \quad (3)$$

where T_0 is the transmittance of the sample before exposure to distilled water, and T_t is the transmittance of the sample after the immersion test was performed.

Pendulum hardness

Hardness was determined according to the standardized test method for König pendulum hardness ASTM D4366-16 (2021) with a Pendulum Hardness Tester (BYK Gardner, Columbia, MD, USA). This test measures the damping time of a normed pendulum disposed on the coating surface. For the König method, the oscillation amplitude from 6 and 3° is recorded, and results are presented as the number of oscillations. The latexes were applied to glass panels at a thickness of 9 mils (*i.e.*, approx. 228 microns), and the films were left to dry for 48 h before measurements were taken. A minimum of three film measurements were acquired for each formula applied to three different panels.

Thermogravimetric analysis (TGA)

The TGA method was used to evaluate the thermal stability of the latex polymers (TGA 851e, Mettler Toledo, Switzerland). Polymer films (around 5 to 10 mg) were heated from ambient temperature to 600 °C at 10 °C/min under a nitrogen atmosphere.

Pyrolysis-gas chromatography-mass spectrometry (Py-GCMS)

This technique is based on the massive alteration by heat of complex structures, such as polymers or copolymers, that gas chromatography cannot directly analyze. Py-GCMS demonstrates the presence of bio-based monomers in the films, as well as the presence of dimers involving bio-based monomers. Mass spectrometry analyses were performed with an integrated system composed of a Pyroprobe and an Agilent Technologies (Santa Clara, CA, USA) CP-3800 gas chromatograph coupled with an Agilent Technologies Saturn 2200 mass spectrometer and equipped with a pyrolysis injection system.

For this analysis, the Pyroprobe settings were carefully selected to provide the necessary thermal conditions for precise sample examination. The set-point temperature was set at 650 °C and maintained for 10 s. The interface temperature, valve oven temperature, and transfer line temperature were all controlled at 250 °C.

RESULTS AND DISCUSSION

Latex Characteristics

The results described in this paper consider that bio-based monomers have equivalent reactivity constants. Indeed, several papers studied the reactivity of monomers IBOMA and THGA with monomers such as BuA and MMA. It is important to recognize the importance of reactivity ratios in copolymerization because they will define the final structure of the copolymers and therefore, their properties. Reactivity ratios, such as r_1 for monomer 1 in the copolymer with monomer 2, define the ratios k11/k12, where k11 is the rate constant for the homopropagation reaction, and k12 is the rate constant for copropagation (Lerari 2015). For example, in the copolymerization of MMA and THGA, the reactivity ratios are comparable to those of MMA with other monomers, such as BuA (Jordan 2021). Similarly, in the copolymerization of MMA and IBOMA, the ratios suggest almost a Bernoullian behavior, *i.e.*, an equal distribution of the monomers (Park *et al.* 2007). Following these studies, we can expect a similar reactivity of these monomers

towards themselves and others. Therefore, these monomers will be considered randomly distributed alongside the polymer chain. In addition, semi-batch polymerization is preferred for the copolymerization of acrylate and methacrylate monomers. It allows better heat control, ensures a safer process, and produces a more homogeneous copolymer despite differences in reactivity ratios (Llorente *et al.* 2022).

Dynamic light scattering (DLS) was used to characterize latexes in terms of particle size and polydispersity index. Then, the solids content was determined using a halogen oven. The solids content results obtained were used to calculate the conversion rate. All data are listed in Table 4.

Table 4. Characteristics of Synthesized Latexes in DLS and Solids Content

Latex	Particle Size (nm)	Polydispersity Index (PDI)	Solids Content (%)	Conversion Rate (%)
M1 *Petrochemical*	117 ± 3	0.30 ± 0.01	24.0 ± 0.2	88.5 ± 0.6
SB2 *Partially-bio-based*	59 ± 1	0.12 ± 0.02	25.9 ± 0.1	98.0 ± 0.4
SB3 *Partially-bio-based*	66 ± 1	0.12 ± 0.02	24.7 ± 0.2	94.7 ±0.7
B1 *Highly Bio-based*	39 ± 1	0.20 ±0.02	24.4 ± 0.1	95.0 ± 0.3

For the petroleum-based latex M1, the particle size found was 117 nm, but for the latexes with bio-based monomers SB2, SB3, and B1, the particle sizes were in the same range, between 39 and 59 nm. No explanation has been found for the larger particle size of M1, but this phenemonene has been observed on different latex batches. While the M1 latex led to a higher particle size than other latexes, these results are consistent with those found in the literature regarding the size (Amaral *et al.* 2005). Llorente *et al.* (2022) obtained a particle size range of 119 to 128 nm for latexes polymerized in batch consisting of IBOMA and 2-octyl acrylate at a solids content of 30%.

The polydispersity index (PDI) measures dispersion homogeneity and ranges from 0 to 1. Values near 0 indicate a homogeneous dispersion, while those greater than 0.3 indicate high heterogeneity. The PDI values for all samples ranged between 0.12 and 0.3, corresponding to relatively homogenous distributions (Eren and Solmaz 2020).

The conversion percent can be calculated using Eq. 2. The conversion was high for all the latexes synthesized, above 88%. However, the conversion for M1 was lower (88.5%) compared to other latexes because the solids content of M1 was 24%. The solids content target in this study was a minimum of 25%. The conversion rate was high for all the latexes synthesised, above 88% (Table 4). Polymerizations are successful in terms of the polydispersity given by the DLS measurement and the conversion rate. The GPC measurements determined the molecular weight of the latexes, which are listed in Table 5. However, the standard deviation was much higher for samples SB3 and B1. Solubility analyses revealed that the THGA monomer was less soluble in THF, which explains the lower M_n of samples SB3 and B1. The molecular weight of samples prepared by miniemulsion is usually very high (Lovell and Schork 2020).

Table 5. Molecular Weight Distribution of Latexes

Latex	Number Average Molecular Weight (Mn) (g/mol)	Weight Average Molecular Weight (Mw) (g/mol)	Polydispersity Index (D)
M1 Petrochemical	850 000 ± 30 000	1 130 000 ± 40 000	1.3 ± 0
SB2 Partially-bio-based	940 000 ± 25 000	1 160 000 ± 35 000	1.2 ± 0.1
SB3 Partially-bio-based	550 000 ± 20 000	1 060 000 ± 120 000	1.9 ± 0.2
B1 Highly Bio-based	425 000 ± 15 000	880 000 ± 140 000	2.1 ± 0.3

Film Characterization

Differential scanning calorimetry (DSC) and minimum film formation temperature (MFFT) analysis

The T_g is one of the most essential factors for coatings. The T_g values met the criteria of an exterior coating to match the intended application. To keep the characteristics of the exterior coating consistent, the copolymer was compounded for a theoretical T_g between 4 and 5 °C. This temperature allowed an equivalent proportion of hard and soft monomers to be maintained. As reported in Table 6, the T_g measured by DSC is compared to the theoretical T_g. The T_g was also compared to MFFT. The MFFT found remains below 10 °C, which is expected for an exterior coating. The MFFT is based on a visual assessment, which can lead to imprecision. However, this measurement is even more essential for the coatings industry than the T_g measurement, as it directly translates to film formation in practice.

Table 6. T_g Calculated *Versus* T_g Measured by DSC According to Samples

Films	Calculated T_g (°C)	Measured T_g by DSC (°C)	MFFT (°C)
M1 *Petrochemical*	4.2	7 ± 2	3
SB2 *Partially -bio-based*	4.6	4 ± 0	2
SB3 *Partially -Bio-based*	4.3	13 ± 0	6
B1 Highly *Bio-based*	4.6	2 ± 1	6

UV-Vis spectroscopy

This analysis aims to quantify film transparency. Transparency is an essential criterion in wood coatings. Indeed, transparent coatings are becoming increasingly popular, as they reveal the natural beauty of wood (Teacă *et al.* 2019). The visible transparency of the prepared acrylic films was studied using a UV-Vis spectrophotometer. Figure 3 shows the percentage of transmittance as a function of wavelength. Measurements were carried out on 300-µm-thick films. This thickness is higher than for regular coating applications, which should be around 100 µm. The films prepared presented a high optical clarity of

over 80% at wavelengths ranging from 500 to 800 nm. A slight decrease was observed between 400 and 500 nm for the SB3 sample. Under normal thickness conditions, the coating, regardless of the sample, would have an optical clarity of over 80%.

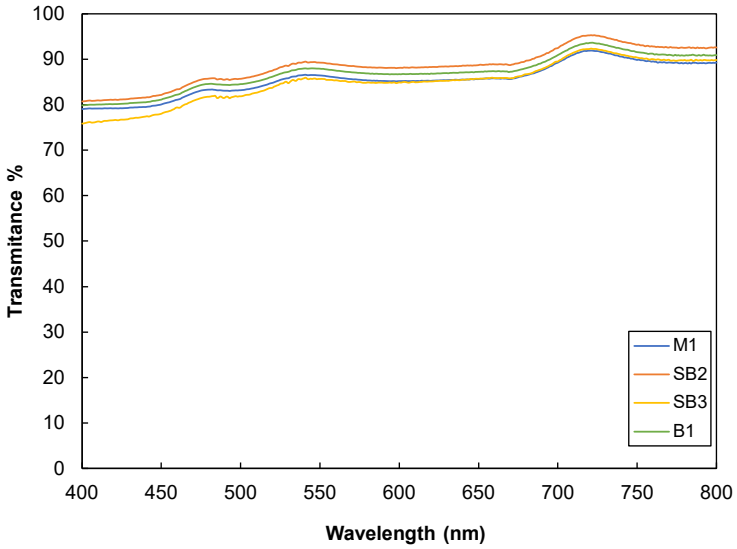

Fig. 3. Transmittance curve obtained by UV-Vis spectrometry for latex films of M1, SB2, SB3, and B1

Gharieh *et al.* (2019) performed a similar analysis on acrylic latex with nanoparticles. They considered transparency to be very good when the transmittance was above 80%. Wang *et al.* (2006) prepared latexes with BuA only; the transparency found was greater than 90% between 400 and 800 nm. Fielding *et al.* (2011) performed optical transparency on acrylic latex films (MMA and BuA). The transmittance curves obtained were similar to those obtained in Fig. 3. The articles cited did not report the thicknesses of the films tested, so it is difficult to make a clear comparison. However, the petrochemical M1 film was used as a reference in this case. The partially-bio-based (SB2 and SB3) and highly bio-based (B1) films follow the same trend in terms of transmittance as the M1 film. In addition, the thickness of 300 µm is high compared to the thickness applied for a coating to protect exterior wood. Thus, it is possible to conclude that coalescence occurred uniformly if the latex was made with bio-based monomers.

Evaluation of water whitening of latex coatings

Figure 4 illustrates the degree of water whitening for various types of latex after 1 h and 24 h of immersion. A general trend of increased whitening between 1 h and 24 h of immersion was observed. This phenomenon can be attributed to the drying process of latex films, during which hydrophilic components, such as emulsifiers migrate to the film surface as water evaporates, leading to whitening. Film M1 appeared to be less susceptible to whitening compared to others, while film B1 seemed to be the most sensitive. Several factors may explain these observations. Firstly, the mass percentage of acrylic acid is higher in SB2 (7.4%) and SB3 (7.5%) latex film, as well as latex film B1 (8%), compared to latex film M1 (7.1%). Whitening is generally more pronounced with higher amounts of acrylic acid, as acrylic acid is a hydrophilic molecule. Furthermore, T_g also influences water whitening. Lower T_g values tend to correlate with increased whitening (Luo and

Huang 2020). In fact, the lower T_g gives the film greater flexibility with greater chain mobility. Film B1 had the lowest T_g at 2 °C, explaining its higher sensitivity to whitening.

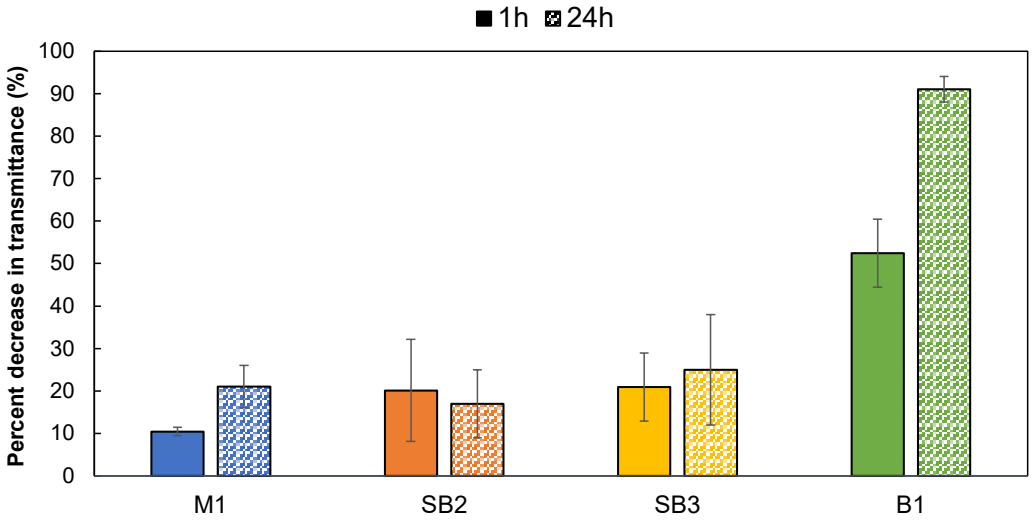

Fig. 4. Degrees of water bleaching for latex films M1, SB2, SB3, and B1 for 1 h and 24 h

Pendulum hardness

Pendulum hardness results are presented in Fig. 5. Latex M1 showed a higher hardness value of 26. For comparison, Pishvaei and Tabrizi (2010) prepared a miniemulsion acrylic latex with a solids content of 40% and a pendulum hardness of 12.

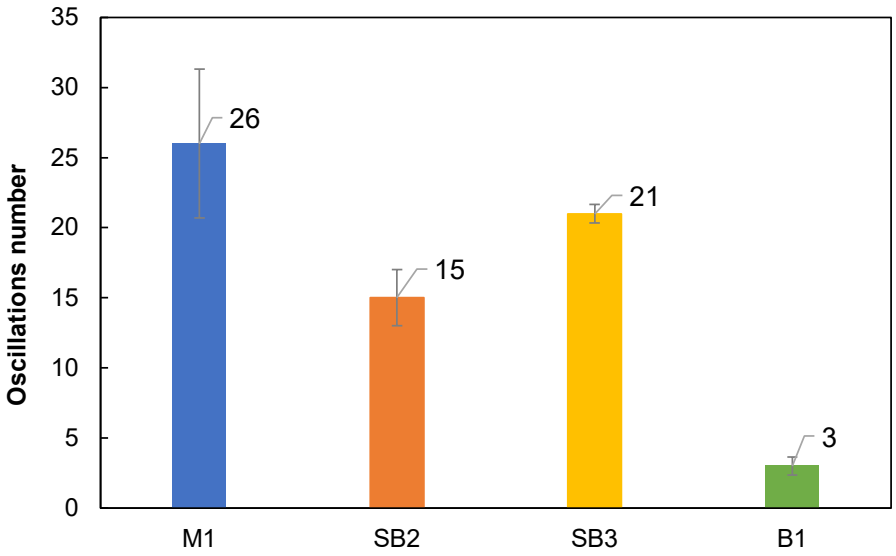

Fig. 5. Pendulum hardness of latex films M1, SB2, SB3, and B1

It is interesting to note that adding a bio-based monomer decreased the hardness of the film. The highly bio-based film B1 remained tacky so that no hardness measurement could be performed. The fact that the film remains tacky is a problem for future applications, as the coating can pick up dirt and dust. The tackiness and softness of B1 also explain the more pronounced whitening demonstrated in the previous analysis. As such,

the monomer quantities must be changed to increase the T_g. Regarding the DSC results, the T_g values obtained for latexes SB2 and B1 were lower than M1 due to a higher proportion of the soft monomer, 55.9% and 60%, respectively. This point may explain the low hardness of B1. It is important to note that a lower T_g usually corresponds to a lower hardness, as the results demonstrated. Through optimizing the monomer composition, it would be possible to achieve a desirable combination of T_g and hardness, thereby improving the film's performance.

Thermogravimetric analysis (TGA) and derivative thermogravimetry (DTG)

Figure 6 shows the thermal degradation characteristics, highlighting noticeable distinctions among the latex films. A one-step degradation process was evident in the case of M1 and SB3 films (devoid of IBOMA). A two-step degradation process was observed for SB2 and B1 films containing IBOMA.

Table 7 presents the specific degradation temperatures in relation to the film type and mass loss. A substantial variance was observed in the temperature at which a 5% mass loss occurred between films with and without IBOMA. The SB2 film exhibited a 5% mass loss at 180 °C, while the M1 and SB3 films exhibited losses at 280 and 272 °C, respectively.

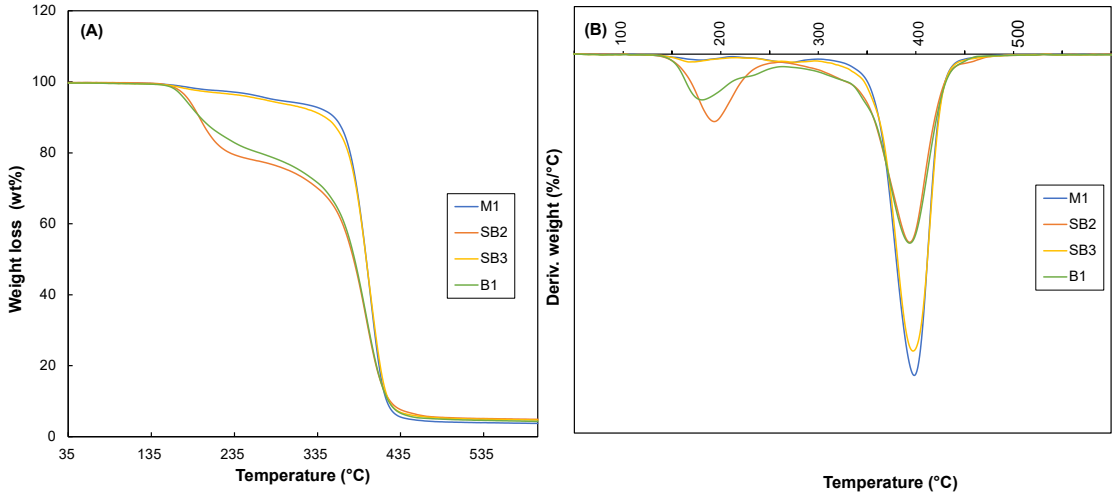

Fig. 6. TGA (A) and DTG (B) for latex films M1, SB2, SB3, and B1

As explained by Fang *et al.* (2020), latexes containing IBOMA display two distinct thermal degradation stages. The initial stage, starting at 196 °C, corresponds to the degradation of isobornyl side chains. Plus, examination of the SB2 and B1 curves shows that the mass lost at the end of the first stage at 335 °C (Fig. 6-A) is in line with the IBOMA quantities quoted in Table 3, *i.e.*, 29% for SB2 and 25% for B1. The second stage, starting at 394 °C, corresponds to the decomposition of the polymer backbone. Nevertheless, the degradation of IBOMA at 196 °C is not detrimental to the intended application. Notably, the maximum degradation temperature remains largely consistent across all films, as detailed in Table 7, with a value of 400 ± 4 °C.

Table 7. TGA and DTG Result of Latex Films M1, SB2, SB3, and B1

Latex	T_5[A] (°C)	T_{15}[A] (°C)	T_{50}[A] (°C)	T_{max1}[B] (°C)	T_{max2}[C] (°C)
M1 Petrochemical	280 ± 5	367 ± 2	395 ± 3		402 ± 5
SB2 Partially-Bio-based	180 ± 1	206 ± 1	378 ± 0	196 ± 1	394 ± 1
SB3 Partially-Bio-based	272 ± 2	363 ± 0	393 ± 1		397 ± 1
B1 Highly Bio-based	175 ± 1	219 ± 1	375 ± 5	181 ± 2	392 ± 2

[A] T_5, T_{15}, and T_{50} are the temperatures at 5%, 15%, and 50% weight loss, respectively
[B] The maximum temperature of the first stage (T_{max1})
[C] The maximum temperature of the second stage (T_{max2})

Pyrolysis-gas chromatography-mass spectrometry (Py-GCMS) analysis

Figure 7 and Tables 8 through 11 show the Py-GCMS results. This analysis aims to verify whether the bio-based monomers are well integrated into the polymer backbone. The results are expressed in the form of several pyrograms. The abscissa corresponds to the retention time. According to the literature, a Py-GCMS pyrogram shows the monomers from 0 to 10 min. Peaks beyond 10 min correspond to dimers and sesquimers (Silva *et al.* 2015). The mass spectra were compared with those of a NIST database, enabling peaks to be assigned and compared.

Figure 7-A and Table 8 correspond to film M1, which contains no bio-based monomers. This pyrogram (in blue) serves as a reference and is overlaid with the pyrogram associated with the other films containing bio-based monomers. Conventional monomers were assigned based on the literature. The peak corresponding to MMA is at 1.5 min, the one corresponding to the BuA is at 6.3 min, and the one at 15 min corresponds to a BuA dimer (Scalarone and Chiantore 2004; Silva *et al.* 2015).

Table 8. *m/z* Majority at the Given Retention Time and Suggested Attribution of Sample M1

Retention Time (min)	*m/z*	Suggested Identification
1.5	69, 41	MMA
3.4	101, 69, 39	MMA-AA dimer
6.4	55, 73	BuA
11.0	97, 69	MMA-BuA dimer
15.0	69, 71	BuA-dimer

In Fig. 7-B, the pyrogram of M1 is superimposed with the pyrogram of SB2 containing the bio-based monomer IBOMA. Two peaks can be attributed to IBOMA, those at 6.4 min and 7.4 min. Thanks to a reverse search with the mass spectrum, the peak at 6.4 min was identified as the terpene ring alone. According to the paper by Yermakov *et al* (2010)., the striking peaks of camphene and its isomers comprising an aliphatic ring are the same as those identified by the analysis, *i.e.*, 93, 91, and 121. Deductively, the peak at 7.4 min corresponds to IBOMA. Two peaks were observed on the pyrogram for the IBOMA monomer. Two degradation stages were observed in DTG for this monomer.

Table 9. *m*/*z* Majority at the Given Retention Time and Suggested Attribution of Sample SB2

Retention Time (min)	*m*/*z*	Suggested Identification
3.2	101, 69	MMA-AA dimer
6.5	83, 97, 70	THGA
6.8	93, 91, 107	Camphene (terpene ring)
7.4	79, 77, 91, 121	IBOMA
11.4	83, 69, 70	IBOMA-THGA dimer
14.0	85, 71, 99	THGA dimer

Figure 7-C corresponds to the superposition of M1 and SB3 containing THGA. The soft part of SB3 is 50% BuA and 50% THGA. A slight shift is observed between the BuA peak at 6.3 min and the peak attributed to THGA at 6.4 min. However, a peak at 14 min appears, which can be attributed to a THGA dimer.

Table 10. *m*/*z* Majority at the Given Retention Time and Suggested Attribution of sample SB3

Retention Time (min)	*m*/*z*	Suggested Identification
3.2	100, 99, 69	MMA-AA dimer
6.2	55, 73	BuA fragment
6.5	97, 83, 70	THGA fragment
10.9	97, 69, 57	MMA-BuA dimer
11.1	85, 83, 69	MMA-THGA dimer
14	85, 71,83	THGA dimer
15	69, 71, 83	BuA dimer

Figure 7-D corresponds to a superposition of film M1 and film B1 containing the two bio-based monomers (IBOMA and THGA). Peaks associated with the bio-based monomers have the same retention time as in the previous pyrograms at 7.4 min, corresponding to IBOMA, 6.4 min for the TGHA monomer, and 14 min for the THGA dimer. However, the terpenic cycle peak no longer appears, as seen in pyrogram B. This is probably due to the larger peak obtained.

Table 11. *m*/*z* Majority at the Given Retention Time and Suggested Attribution of sample B1

Retention Time (min)	m/z	Suggested Identification
3.2	101, 69	MMA-AA dimer
6.5	83, 97, 70	THGA
6.8	93, 91, 107	Camphene (terpene ring)
7.4	79, 77, 91, 121	IBOMA
11.4	83, 69, 70	IBOMA-THGA dimer
14.0	85, 71, 99	THGA dimer

As shown in Tables 9 through 12, beyond 10 min, the variation in *m*/*z* can be attributed to differences in dimer structures that arise from variations in the utilized monomers. However, reported majority *m*/*z* were still similar between the films. In conclusion, this analysis shows that bio-based monomers had been incorporated into the copolymers that was formed.

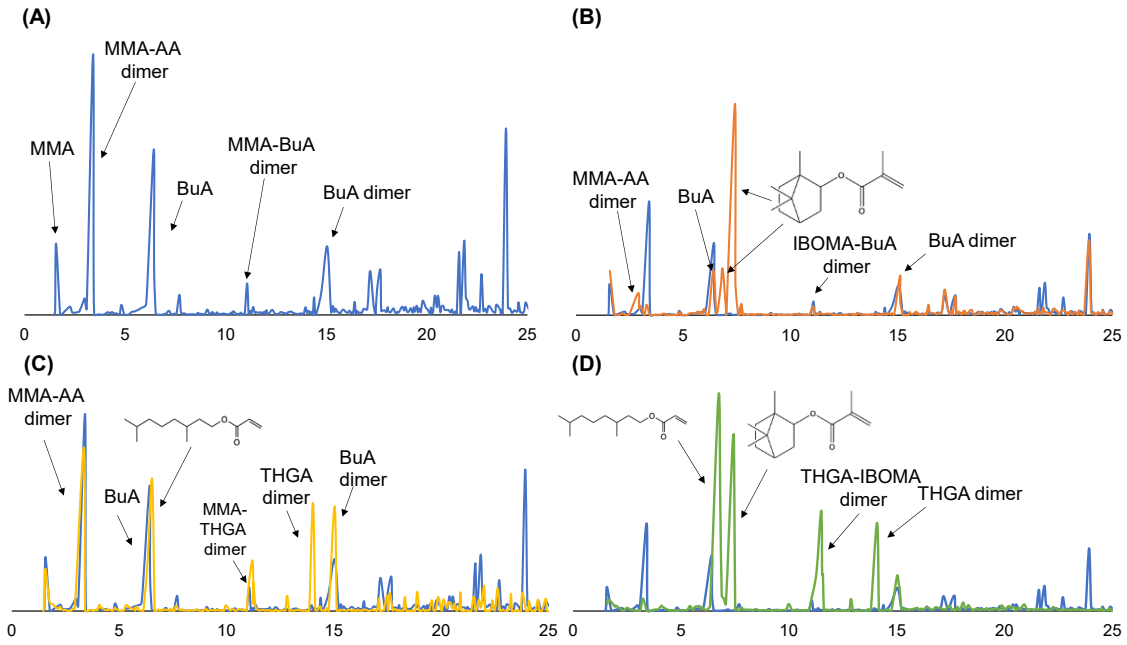

Fig. 7. Pyrolysis-GCMS pyrograms: A - Pyrogram of film M1 (petrochemical), B - Pyrogram of the SB2 film (partially-bio-based) superimposed on the M1 film (petrochemical), C - Pyrogram of the SB3 (partially-bio-based) film superimposed with the M1 (petrochemical), and D - Pyrogram of film B1 (Highly bio-based) superimposed on M1 (petrochemical)

CONCLUSIONS

1. Terpenes represent a potential sustainable alternative to petrochemicals. This study suggests that (meth)acrylated terpenes can function as conventional monomers, with isobornyl methacrylate (IBOMA) and tetrahydrogeraniol acrylate (THGA) showing potential as substitutes for methylmethacrylate (MMA) and butyl acrylate (BuA), respectively. Future research should explore the transformation of pinenes, which share a similar chemical structure with IBOMA and are more abundant in turpentine, to further uncover the potential of terpenes
2. The successful synthesis of latex was underscored by the uniformity of droplets, as shown by the dynamic light scattering findings. Furthermore, thermogravimetric and Pyrolysis-Gas Chromatography-Mass Spectrometry analysis confirmed the successful integration of these bio-based monomers into the films and showed the presence of dimers. The measured T_g *via* DSC remained consistent with the calculated T_g.
3. Latexes with bio-based monomers exhibited optical properties comparable to traditional films, as demonstrated by transparency tests. Better management of the amount of acrylic acid and adjusting the targeted T_g could enhance latex performance

in terms of water whitening resistance and pendulum hardness. Additionally, assessing the performance of latexes with bio-based monomers when applied to wood substrates is essential for future research.

ACKNOWLEDGMENTS

The authors are grateful to Jérémy Winninger and Ingrid Calvez for their valuable assistance. Thanks to Yves Bédard, Gabrielle Raiche-Marcoux, and François Otis for their help with the various analyses. The authors would also like to thank the members of the Centre for Research on Renewable Materials (CRMR), the NSERC Industrial Chair on Sustainable Wood Construction (CIRCERB), and its industrial partners.

Funding Sources

The authors are grateful to the Natural Sciences and Engineering Research Council of Canada for the financial support through its IRC, and CRD programs (IRCPJ 461745-18 and RDCPJ 524504-18) as well as the industrial partners of the NSERC industrial chair on eco-responsible wood construction (CIRCERB).

Author Contributions

MC carried out most of the experimental part of this work and wrote the manuscript. SB carried out some of the experiments and contributed its expertise in analytical chemistry. YE supported the writing of the manuscript. VL supported the manuscript writing and supervised the project.

Conflicts of Interest

The authors declare that there is no conflict of interest. The funders had no role in the study's design; the collection, analysis, or interpretation of data; the writing of the manuscript; or the decision to publish the results.

REFERENCES CITED

Allasia, M., Aguirre, M., Gugliotta, L. M., Minari, R. J., and Leiza, J. R. (2022). "High bio-based content waterborne latexes stabilized with casein," *Progress in Organic Coatings* 168, article ID 106870. DOI: 10.1016/j.porgcoat.2022.106870

Amaral, d. M., Roos, A., Asua, J. M., and Creton, C. (2005). "Assessing the effect of latex particle size and distribution on the rheological and adhesive properties of model waterborne acrylic pressure-sensitive adhesives films," *Journal of Colloid and Interface Science* 281(2), 325-338. DOI: 10.1016/j.jcis.2004.08.142

Anastas, P., and Eghbali, N. (2010). "Green chemistry: Principles and practice," *Chemical Society Reviews* 39(1), 301-312. DOI: 10.1039/B918763B

ASTM D4366-16 (2021) "Standard test methods for hardness of organic coatings by pendulum damping tests," ASTM International, West Conshohocken, PA, USA.

Badía, A., Movellan, J., Barandiaran, M. J., and Leiza, J. R. (2018). "High bio-based content latexes for development of sustainable pressure sensitive adhesives," *Industrial and Engineering Chemistry Research* 57(43), 14509-14516. DOI: 10.1021/acs.iecr.8b03354

Baek, S.-S., Jang, S.-H., and Hwang, S.-H. (2017). "Construction and adhesion performance of biomass tetrahydro-geraniol-based sustainable/transparent pressure sensitive adhesives," *Journal of Industrial and Engineering Chemistry* 53, 429-434. DOI: 10.1016/j.jiec.2017.05.017

Belgacem, M. N., and Gandini, A. (2011). *Monomers, Polymers and Composites from Renewable Resources*, Elsevier, Amsterdam, Netherlands.

Castagnet, T., Aguirre, G., Asua, J. M., and Billon, L. (2020). "Bioinspired enzymatic synthesis of terpenoid-based (meth)acrylic monomers : A solvent-, metal-, amino-, and halogen-free approach," *ACS Sustainable Chemistry and Engineering* 8(19), 7503-7512. DOI: 10.1021/acssuschemeng.0c02307

Demurtas, O. C., Nicolia, A., and Diretto, G. (2023). "Terpenoid transport in plants: How far from the final picture?," *Plants* 12(3), article 634. DOI: 10.3390/plants12030634

Désor, D., Krieger, S., Apitz, G., and Kuropka, R. (1999). "Water-borne acrylic dispersions for industrial wood coatings," *Surface Coatings International* 82(10), 488-496. DOI: 10.1007/BF02692644

Donoso, D., Ballesteros, R., Bolonio, D., García-Martínez, M.-J., Lapuerta, M., and Canoira, L. (2021). "Hydrogenated turpentine: A bio-based component for jet fuel," *Energy & Fuels* 35(2), 1465-1475. DOI: 10.1021/acs.energyfuels.0c03379

Droesbeke, M. A., Simula, A., Asua, J. M., Du Prez, F., Melnikov, F., Lam, C. H., Lounsbury, A. W., Mellor, K. E., Janković, N. Z., Tu, Q., *et al.* (2018). "Biosourced terpenoids for the development of sustainable acrilic pressure-sensitive adhesives *via* emulsion poymerisation," *Green Chemistry* 20(9), 1929-1961. DOI: 10.1039/C8GC00482J

Eren, B., and Solmaz, Y. (2020). "Preparation and properties of negatively charged styrene acrylic latex particles cross-linked with divinylbenzene," *Journal of Thermal Analysis and Calorimetry* 141(4), 1331-1339. DOI: 10.1007/s10973-019-09121-8

Fang, C., Zhu, X., Cao, Y., Xu, X., Wang, S., and Dong, X. (2020). "Toward replacement of methyl methacrylate by sustainable bio-based isobornyl methacrylate in latex pressure sensitive adhesive," *International Journal of Adhesion and Adhesives* 100, article ID 102623. DOI: 10.1016/j.ijadhadh.2020.102623

Fielding, L. A., Tonnar, J., and Armes, S. P. (2011). "All-acrylic film-forming colloidal polymer/silica nanocomposite particles prepared by aqueous emulsion polymerization," *Langmuir* 27(17), 11129-11144. DOI: 10.1021/la202066n

Fox, T. G. (1956). "Influence of diluent and of copolymer composition on the glass temperature of a polymer system," *Bulletin of the American Physical Society* 1, 123.

Gharieh, A., Mirmohseni, A., and Khorasani, M. (2019). "Preparation of UV-opaque, vis-transparent acrylic–silica nanocomposite coating with promising physico-mechanical properties via miniemulsion polymerization," *Journal of Coatings Technology and Research* 16(3), 781-789. DOI: 10.1007/s11998-018-00155-5

González, E., Stuhr, R., Vega, J. M., García-Lecina, E., Grande, H.-J., Leiza, J. R., and Paulis, M. (2021). "Assessing the effect of CeO_2 nanoparticles as corrosion inhibitor in hybrid bio-based waterborne acrylic direct to metal coating binders," *Polymers* 13(6), article 848. DOI: 10.3390/polym13060848

González-Laredo, R. F., Rosales-Castro, M., Rocha-Guzmán, N. E., Gallegos, J. A., Moreno-Jiménez, M. R., and Karchesy, J. J. (2015). "Preservación de la madera usando productos naturales," *Madera y Bosques* 21, 63-76. DOI : 10.21829/myb.2015.210427

Hadjichristidis, N., Mays, J., Ferry, W., and Fetters, L. J. (1984). "Properties and chain flexibility of poly (dl-isobornyl methacrylate)," *Journal of Polymer Science: Polymer Physics Edition* 22(10), 1745-1751. DOI : 10.1002/pol.1984.180221004

Izmest'ev, E. S., Rubtsova, S. A., and Kutchin, A. V. (2019). "Environmental aspects of sulfate turpentine refining (review)," *Theoretical and Applied Ecology* 1, 12-22. DOI: 10.25750/1995-4301-2019-1-012-022

Jiao, C., Sun, L., Shao, Q., Song, J., Hu, Q., Naik, N., and Guo, Z. (2021). "Advances in waterborne acrylic resins : Synthesis principle, modification strategies, and their applications," *ACS Omega* 6(4), 2443-2449. DOI: 10.1021/acsomega.0c05593

Jones, F. N., Nichols, M. E., and Pappas, S. P. (2017). *Organic Coatings: Science and Technology*, Fourth Edition, John Wiley and Sons, Inc., Hoboken, NJ, USA.

Jordan, B. (2021). *Synthesis of Random and Block Copolymers from Terpene-Based and Acrylate-Based Monomers*, Doctoral dissertation, University of Nottingham, Nottingham, England.

Lerari, D. (2015). "Synthesis and characterization of new copolymer based cinnamyl methacrylate monomer : Determination of monomer reactivity ratio and statistical sequence," *Materials Research* 18, 1008-1014. DOI: 10.1590/1516-1439.012015

Lippke, B., Oneil, E., Harrison, R., Skog, K., Gustavsson, L., and Sathre, R. (2011). "Life cycle impacts of forest management and wood utilization on carbon mitigation : Knowns and unknowns," *Carbon Management* 2(3), 303-333. DOI: 10.4155/cmt.11.24

Llorente, O., Barquero, A., Paulis, M., and Leiza, J. R. (2022). "Challenges to incorporate high contents of bio-based isobornyl methacrylate (IBOMA) into waterborne coatings," *Progress in Organic Coatings* 172, article ID 107137. DOI: 10.1016/j.porgcoat.2022.107137

Lovell, P. A., and Schork, F. J. (2020). "Fundamentals of emulsion polymerization," *Biomacromolecules* 21(11), 4396-4441. DOI: 10.1021/acs.biomac.0c00769

Luo, Z., and Huang, H. (2020). "Glass-transition temperature of a polyacrylate latex film and its water whitening resistance," *Journal of Applied Polymer Science* 137(6), article ID 48361. DOI: 10.1002/app.48361

Machotová, J., Černošková, E., Honzíček, J., and Šňupárek, J. (2018). "Water sensitivity of fluorine-containing polyacrylate latex coatings: Effects of crosslinking and ambient drying conditions," *Progress in Organic Coatings* 120, 266-273. DOI: 10.1016/j.porgcoat.2018.03.016

Noppalit, S., Simula, A., Ballard, N., Callies, X., Asua, J. M., and Billon, L. (2019). "Renewable terpene derivative as a biosourced elastomeric building block in the design of functional acrylic copolymers," *Biomacromolecules* 20(6), 2241-2251. DOI: 10.1021/acs.biomac.9b00185

Park, S. I., Lee, S. I., Hong, S.-J., and Cho, K. Y. (2007). "Suspension polymerization and characterization of transparent poly(methyl methacrylate-co-isobornyl methacrylate)," *Macromolecular Research* 15(5), 418-423. DOI: 10.1007/BF03218808

Pishvaei, M., and Tabrizi, F. F. (2010). "Synthesis of high solid content polyacrylate/nanosilica latexes via miniemulsion polymerization," *Iranian Polymer Journal* 19(9), 707-716.

Sainz, M. F., Souto, J. A., Regentova, D., Johansson, M. K. G., Timhagen, S. T., Irvine, D. J., Buijsen, P., Koning, C. E., Stockman, R. A., and Howdle, S. M. (2016). "A facile and green route to terpene derived acrylate and methacrylate monomers and

simple free radical polymerisation to yield new renewable polymers and coatings," *Polymer Chemistry* 7(16), 2882-2887. DOI: 10.1039/C6PY00357E

Scalarone, D., and Chiantore, O. (2004). "Separation techniques for the analysis of artists' acrylic emulsion paints," *Journal of Separation Science* 27(4), 263-274. DOI: 10.1002/jssc.200301638

Silva, M. F., Doménech-Carbó, M. T., and Osete-Cortina, L. (2015). "Characterization of additives of PVAc and acrylic waterborne dispersions and paints by analytical pyrolysis–GC–MS and pyrolysis–silylation–GC–MS," *Journal of Analytical and Applied Pyrolysis* 113, 606-620. DOI: 10.1016/j.jaap.2015.04.011

Sun, X., Qian, Z., Luo, L., Yuan, Q., Guo, X., Tao, L., Wei, Y., and Wang, X. (2016). "Antibacterial adhesion of poly(methyl methacrylate) modified by borneol acrylate," *ACS Applied Materials and Interfaces* 8(42), 28522-28528. DOI: 10.1021/acsami.6b10498

Teacă, C.-A., Roşu, D., Mustaţă, F., Rusu, T., Roşu, L., Roşca, I., and Varganici, C.-D. (2019). "Natural bio-based products for wood coating and protection against degradation: A Review," *BioResources* 14(2), 4873-4901. DOI: 10.15376/biores.14.2.Teaca

Ulrich, R. S. (1983). "Aesthetic and affective response to natural environment," in: *Behavior and the Natural Environment*, Vol. 6, Springer Publishing Company, New York City, NY, USA, pp. 85-125. DOI: 10.1007/978-1-4613-3539-9_4

Wang, T., Lei, C. -H., Dalton, A. B., Creton, C., Lin, Y., Fernando, K. A. S., Sun, Y. -P., Manea, M., Asua, J. M., and Keddie, J. L. (2006). "Waterborne, nanocomposite pressure-sensitive adhesives with high tack energy, optical transparency, and electrical conductivity," *Advanced Materials* 18(20), 2730-2734. DOI: 10.1002/adma.200601335

Yermakov, A. I., and Khlaifat, A. L. (2010). "Characteristics of the GC-MS mass spectra of terpenoids (C10H16)," *Chemical Sciences Journal* 2010, 1-10. DOI: 10.4172/2150-3494.1000005

Zhang, B., Ma, Y., Chen, D., Xu, J., and Yang, W. (2013). "Preparation of poly (styrene-co-isobornyl methacrylate) beads having controlled glass transition temperature by suspension polymerization," *Journal of Applied Polymer Science* 129(1), 113-120. DOI:10.1002/app.38710

Article submitted: May 29, 2024; Peer review completed: July 11, 2024; Revised version received: July 15, 2025; Accepted: July 17, 2024; Published: July 24, 2024.
DOI: 10.15376/biores.19.3.6510-6529